

REVIEW ARTICLE

Imaging of the unusual pediatric ‘blastomas’

Georgia Papaioannou^{a,b}, Neil J. Sebire^c and Kieran McHugh^a

^aDepartment of Radiology, Great Ormond Street Hospital, Great Ormond Street, London, WC1N 3JH, UK;

^bDepartment of Radiology, Mitera Hospital, 6 Erythrou Stavrou Str, 1515 23 Marousi, Athens, Greece;

^cDepartment of Histopathology, Great Ormond Street Hospital, Great Ormond Street, London, WC1N 3JH, UK

Corresponding address: G. Papaioannou, MD, Department of Radiology, Great Ormond Street Hospital, Great Ormond Street, London, WC1N 3JH, UK. Email: gpapaio@hotmail.com

Date accepted for publication 1 December 2008

Abstract

‘Blastomas’ are tumors virtually unique to childhood. Controversy surrounds their nomenclature and there is no globally accepted classification. They are thought to arise from immature, primitive tissues that present persistent embryonal elements on histology, affect a younger pediatric population and are usually malignant. The ‘commoner’ blastomas (neuroblastoma, nephroblastoma, hepatoblastoma, medulloblastoma) account for approximately 25% of solid tumors in the pediatric age range. We present examples of the more unusual blastematosus pediatric tumors (lipoblastoma, osteoblastoma, chondroblastoma, hemangioblastoma, gonadoblastoma, sialoblastoma, pleuropulmonary blastoma, pancreatoblastoma, pineoblastoma, and medulloblastoma) that were recorded in our institution. Although these rare types of blastomas individually account for <1% of pediatric malignancies, collectively they may be responsible for up to 5% of pediatric tumors in a given population of young children. Imaging is often non-specific but plays an important role in their identification, management and follow-up. Some characteristic imaging features at diagnosis, encountered in cases diagnosed and treated in our institution, are described and reviewed.

Keywords: *Blastomas; diagnostic imaging; child.*

Introduction

The majority of pediatric cancers reflect an abnormal developmental process, an ‘error’ in the chromatic structure, and to a lesser degree result from external insult or exposure^[1]. The suffix ‘blastoma’ reflects a presumed relationship to primitive, ‘blastic’ elements^[2] and a dysontogenetic character^[3]. The pediatric embryonal tumors are presumed to arise from immature cellular populations that have not completed the process of differentiation to mature tissue phenotype during pre- and post-natal development and are diagnosed in the majority during the first 5 years of life^[1].

The four commonest embryonal malignancies (neuroblastoma, retinoblastoma, nephroblastoma (Wilms’ tumor), and hepatoblastoma) represent the most frequent solid neoplasms presenting in early childhood; they account for approximately 20% of malignancy in children younger than 15 years^[1]. Medulloblastoma, in addition, is the commonest malignant central nervous system (CNS) tumor of childhood^[4].

In this review, we present the radiologic features of the less common blastematosus tumors of childhood according to their prevalence (lipoblastoma, osteoblastoma, chondroblastoma, hemangioblastoma, gonadoblastoma, sialoblastoma, pleuropulmonary blastoma, pancreatoblastoma, pineoblastoma, and medulloblastoma) that were recorded in our institution. Since these tumors individually account for <1% of the pediatric malignancies, radiologists may only encounter isolated cases. However, some specific or suspicious features presented in this paper could help them include these entities in their differential diagnosis.

Lipoblastomas

These are rare benign adipose tumors arising from immature adipocytes demonstrating varying degrees of differentiation^[5,6]. Lipoblastomas show male predominance and are found almost exclusively in children younger than 5 years; 12 months is the reported median age of presentation with some cases present at birth^[5–7].

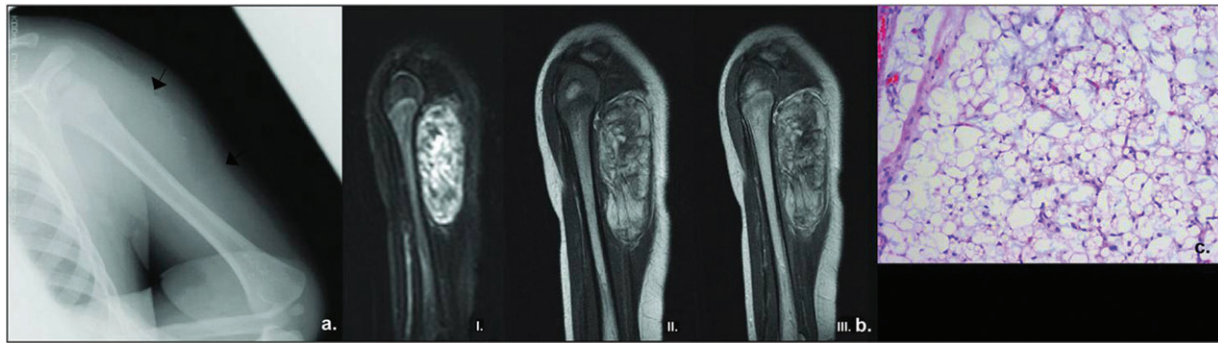


Figure 1 A 4-month-old girl with lipoblastoma of the left arm presented with swelling. (a) Plain film of the left arm reveals a soft tissue mass (arrows) in the posterolateral portion of the arm with no abnormalities in the adjacent humerus. (b) Sagittal MRI views of the left arm. A well-circumscribed, heterogeneous mass is seen within the left triceps, separate from the humerus and subcutaneous tissues. On turbo short tau inversion recovery (STIR) image (I), there is no surrounding edema – an indicator of slow growth. On T1W SE image (II), areas of high signal intensity are seen within the lesion, suggesting presence of fat which shows however slightly lower signal intensity than that of subcutaneous fat and minor enhancement on T1W spin echo post-contrast image (III). (c) Photomicrograph demonstrating a lobule within the lesion composed of adipocytes and numerous lipoblasts with central ‘scalloped’ nucleus and vacuolated cytoplasm. There is no nuclear atypia (H&E, original magnification $\times 100$).

There are two forms of lipoblastoma: (a) the lipoblastoma – a superficial, well circumscribed, and encapsulated lesion, which macroscopically resembles a lipoma; (b) the lipoblastomatosis – a deeply located, poorly circumscribed, macroscopically diffuse and infiltrative lesion. Lipoblastomatosis is commoner, affecting 66% of all cases^[8], and has a tendency to recur post-surgically^[5,6].

Lipoblastomas present as soft, non-tender, lobular masses of variable size, which enlarge rapidly^[5,6]. They usually occur in the extremities, followed by the chest wall and the retroperitoneum, and very rarely in the mediastinum (Figs. 1–3). A few reports of intrascrotal lipoblastomas mimicking testicular torsion have been made^[9]. These tumors show a peculiar predilection for the left side of the body, which may suggest an association with genes of asymmetry, and a breakpoint on chromosome 8q 11–13^[5].

Plain radiographs show a non-specific soft-tissue mass with no calcifications and no erosion of the adjacent bones (Fig. 1). On ultrasound (US), the lesion is lobulated, of mixed echogenicity. With large lesions, adjacent structures are usually displaced but not significantly compressed (Figs. 2 and 3). The lipomatous features of the lesion, which strongly depend on the amount of mature lipocytes^[5,6], are usually evident on computed tomography (CT) and magnetic resonance imaging (MRI) where a detailed map of its location and extent is provided (Figs. 2 and 3). The increased cellularity of lipoblastomas makes their appearances on MRI confusing, as they show high signal on both T1-weighted (T1W) and T2-weighted (T2W) images but the signal on T1W is lower and often more heterogeneous than that of the ‘mature’

subcutaneous fat (Figs. 1 and 2). This feature may differentiate lipoblastomas from lipomas.

Treatment of lipoblastomas is complete surgical excision, with recurrence rates that range from 9% to 22%, usually associated with incomplete excision^[7].

Osteblastomas

These are relatively uncommon benign bone neoplasms, with a tendency to affect the vertebral column with a predilection for the posterior spinal elements^[10]. Ninety percent of osteblastomas present during the first two decades of life with a range of 6 months to 75 years^[11]. There is a male predominance with non-specific symptoms, such as dull aching pain and localized tenderness at the lesion site, or myelopathic signs when they invade intra-spinally^[11]. In children, altered gait patterns or reactive scoliosis may be encountered. None of the available series specifically addresses the differences between the pediatric and adult patient populations^[12].

Osteoblastoma is twenty times less common in occurrence than osteosarcoma and four times less frequent than osteoid osteoma^[11]. It has also been termed ‘giant osteoid osteoma’ because of their striking histologic similarity, although radiologically they are very different as osteoblastoma tends to form a less sclerotic, more expansile mass which may acquire a large size due to delayed diagnosis^[11,13].

Usually CT is the examination of choice offering detailed information about the origin, extent and nature of the tumor^[14]. Spinal osteoblastoma is usually a well-defined, expansile lytic bone lesion with a sclerotic rim and a central portion with granular appearance

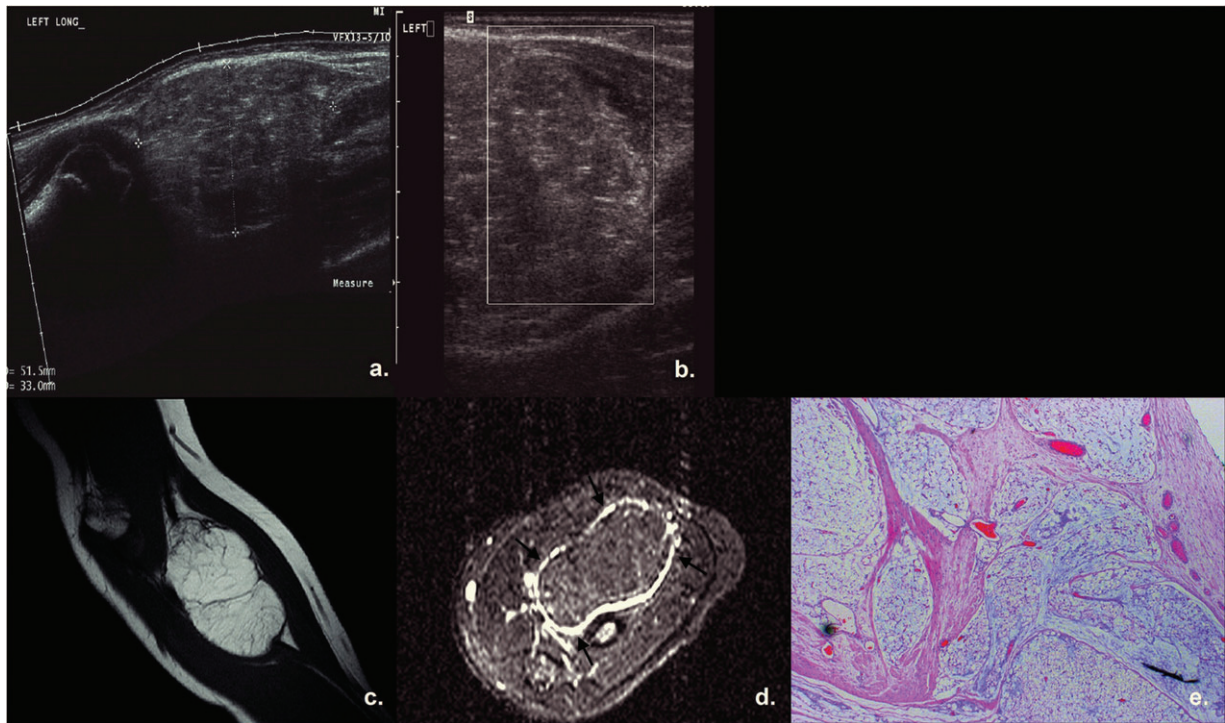


Figure 2 An 8-year-old girl presented with 'cystic' swelling of the left forearm due to lipoblastoma. Ultrasound (extended longitudinal view (a), sagittal view (b)) revealed a slightly lobulated heterogeneous mass of low vascularity (b), in close proximity to muscles. On MRI images, the lobulated lesion did not exhibit any aggressive features, appeared as high signal on T1W (c) and suppressed signal on STIR (d), suggesting the presence of fat. Prominent symmetrically distributed vessels in the periphery of the lesion became evident on axial STIR images (arrows) (d). (e) Low power photomicrograph demonstrating the lobulated nature of the tumor with fatty lobules separated by fibrous septae (H&E, original magnification $\times 20$).



Figure 3 A 13-month-old girl presented with an abdominal mass due to an abdominal lipoblastoma. Ultrasound (a) revealed a large echogenic lesion in the central abdomen (arrows) which displaced liver cephalad (I, sagittal view) but caused no obstruction to the right kidney (RK) (II, axial view). (b) CT of the abdomen demonstrated a large well-defined hypodense, slightly heterogeneous, mesenteric mass which displaced the liver superiorly (I, sagittal view) but caused no compression to the aorta (arrows) (II, axial view).

due to punctate mineralization of the osteoid (Fig. 4)^[11]. It may show locally aggressive features, and recur post-operatively^[13]. MRI rarely contributes to the diagnosis as features are non-specific, sometimes confusing, and there is usually overestimation of the tumor extent due to widespread inflammatory reaction^[13–15].

Treatment of osteoblastomas includes wide surgical excision with autogenous bone grafting if necessary (Fig. 4).

Chondroblastomas

They are rare benign cartilaginous neoplasms which typically develop from cartilage germ cells of the epiphysis of skeletally immature patients and account for less than 1% of all bone neoplasms^[13,16–20]. Chondroblastoma typically develops in the long bones of young males with a peak incidence around the

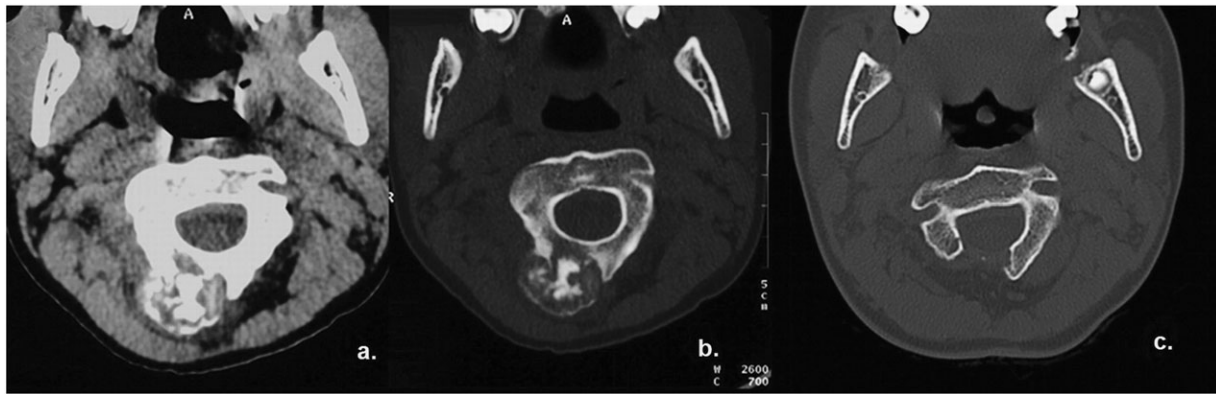


Figure 4 A 12-year-old boy with osteoblastoma of the cervical spine presented with neck pain. CT of the neck (a,b) revealed an exophytic, well-defined, expansile bony lesion arising from the right posterior arch of C2. The peripheral sclerotic rim and matrix calcification due to punctate mineralization of the osteoid were better seen on bony algorithm images (b). This lesion was treated surgically with right laminectomy (c).

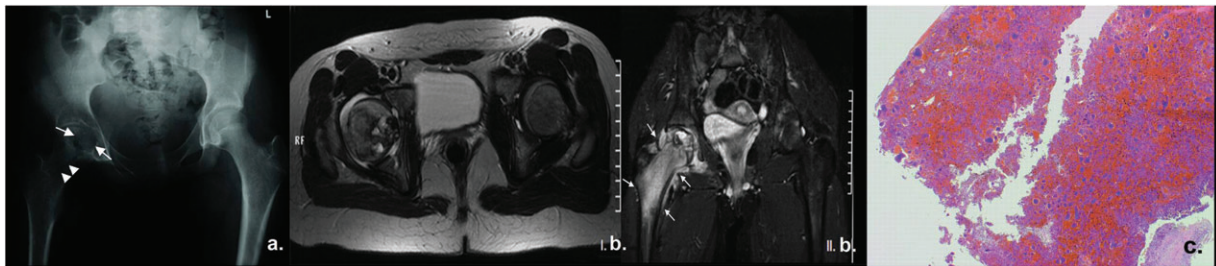


Figure 5 A 14-year-old girl presented with pain and limited range of motion of the right hip joint due to chondroblastoma of the femoral head. (a) Plain film of the pelvis demonstrated an expansile, lobulated, lytic lesion (arrows) in proximal epiphysis of the right femur with matrix punctate calcification. Note is made of a prior biopsy needle tract (arrowheads). (b) On MRI, the lesion presented a heterogeneous high signal on T2W axial images (I) with small, widely scattered foci of higher signal intensity. In addition, extensive inflammatory reaction in the proximal part of the femur and adjacent soft-tissues is noted on coronal T2W images with fat suppression (arrows) (II). (c) Photomicrograph demonstrating numerous ovoid chondroblasts with bland nuclei within a hemorrhagic background admixed with numerous osteoclast-like giant cells indicating chondroblastoma (H&E, original magnification $\times 100$).

second decade of life^[21]. The most frequent sites of involvement are the proximal parts of the humerus and tibia and the proximal and distal parts of the femur, and rarely the spine^[17,20,22,23]. Chondroblastoma of the spine behaves more aggressively than those in long bones, with high recurrence and mortality rates^[22]. Chondroblastomas usually arise from a secondary ossification center which is a unique location for primary bone tumors^[20,21]. Sixty percent of chondroblastomas cross the growth plate to extend into the metaphysis^[13,18].

Clinical presentation usually includes quite severe local pain, swelling and limited range of motion of the adjacent joint^[21]. Chondroblastoma is generally benign, shows slow pattern of growth with well-defined margins, but its clinical course is unpredictable as aggressive behavior with local recurrence and lung metastases have been reported^[16,19,23]. The recurrence rate ranges from 10% to 35% after curettage and reconstruction with either bone graft or polymethylmethacrylate

bone cement^[20]. Factors contributing to recurrence are debatable among studies; more recent reports include: young age, aneurysmal bone cyst components, aggressiveness, anatomic site and inadequate surgery^[20,22]. The suspicion that an open growth plate negatively impacts local recurrence has not been proven^[20].

On plain radiographs, chondroblastoma appears as an expansile, lobulated, lytic lesion in the epiphysis (Fig. 5a)^[20]; it often shows matrix punctate calcification which is better demonstrated on CT^[13,21]. In aggressive cases, destruction of the cortex may be seen but this is generally unusual^[16]. On MRI, chondroblastoma shows low or intermediate signal intensity on T1W images. T2W images demonstrate internal heterogeneity with often small, widely scattered foci of higher signal intensity on gradient-recalled imaging, which correspond to foci of hyaline cartilage or aneurysmal bone cyst (Fig. 5b)^[13,16]. Prominent soft tissue and regional bone marrow edema and periosteal reaction may coexist (Fig. 5bII)^[13].

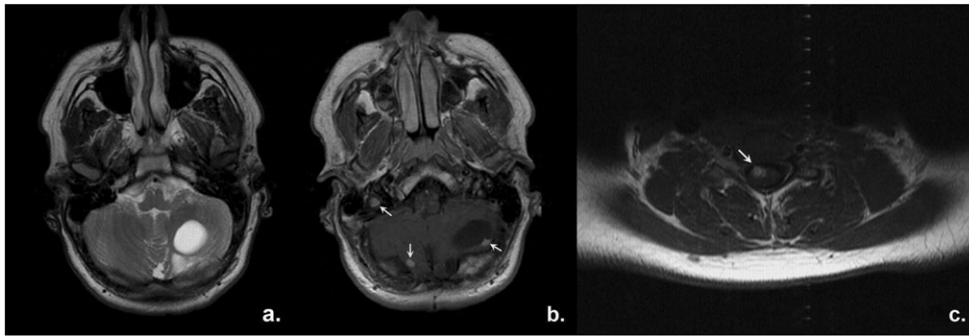


Figure 6 A 15-year-old boy with Von-Hippel–Lindau’s disease. Axial MRI images of brain and spine. On T2W images (a), the cystic portion of a large hemangioblastoma in the left cerebellar hemisphere is easily identified. T1W post gadolinium images reveal several mural enhancing nodules (arrows) which all represent cerebellar hemangioblastomas (b) as well as one spinal hemangioblastoma (c, arrow).

Post gadolinium administration, there is mild enhancement of the tumor and more marked enhancement of the adjacent inflammatory regions in the bone marrow, soft tissues and periosteum^[13].

Since chondroblastoma typically develops in the epiphyseal zone, en bloc resection strategy is usually adopted with sacrifice of the joint function and inevitable growth disturbance^[19].

Hemangioblastomas

They are usually benign tumors that occur in young adults and children with Von-Hippel–Lindau’s disease, in whom they tend to be multiple and associated with the presence of cysts and tumors in other viscera, angiomas of the retina and polycythaemia^[24]. Despite the implication of primitive, aggressive origin they are not malignant primitive neuroectodermal tumors (PNETs), but very low-grade, indolent vascular neoplasms with uniform cellular structure, extremely low mitotic activity and little pleomorphism^[24], classified as WHO grade I^[2].

Hemangioblastomas are usually infra-tentorial, located in the cerebellum or in the brainstem, at the area postrema. About 70% of cerebellar hemangioblastomas and 20% of those located in the cerebrum and the brain stem are cystic with a small mural nodule attached onto the cystic wall^[24]. The wall of the cyst is composed of fibrillary neuroglia and is devoid of tumor. On CT and MRI, hemangioblastomas present as cystic lesions with a mural enhancing nodule (Fig. 6)^[25]. Although hemangioblastomas show no tendency to metastasize, there are sporadic reports of intra-spinal dissemination and local recurrence possibly due to subtotal excision^[24].

Gonadoblastomas

They occur in the perinatal period and represent the least common type of germ cell tumors, deriving from primordial germ cells^[26]. Gonadoblastomas are almost exclusively found in phenotypic sex-reversed females



Figure 7 A 10-year-old girl with an abdominal mass due to gonadoblastoma. CT of the abdomen post injection of contrast showed a large heterogeneous soft-tissue mass which occupied the pelvis and displaced the uterus posteriorly (arrow). A small amount of fluid is noted behind the uterus.

with gonadal dysgenesis associated with a Y chromosome, or Y chromosome fragment (cell line) in their genome (XY females)^[26–30]. There are a few reports of gonadoblastoma development in anatomically male children with cryptorchism, sliding testicle, hypospadias, and even normal scrotal testicles and in dysgenetic ovaries in the apparent absence of Y chromosome^[29,30].

Although gonadoblastoma per se is a benign tumor and does not metastasize, there is potential for transformation into malignant germ cell tumors, usually a combination of gonadoblastoma and seminoma, which makes the prognosis less favorable^[29,30].

Gonadoblastomas may represent microscopic neoplasms, too small to be detected by diagnostic imaging. When obvious macroscopically, ovaries with gonadoblastoma development have the appearance of solid tumors in the lower abdomen on US and CT while some cases with bloody ascites have been reported^[29] (Fig. 7).

Testicular gonadoblastoma on US presents as a hyperechoic area in the central part of the affected testicle^[30].

Treatment of gonadoblastomas is gonadectomy, which leads to cure^[26,30]. In the presence of abnormal or undescended contralateral gonad, bilateral gonadectomy is recommended since the incidence of bilaterality of gonadoblastoma is considered high^[30].

Sialoblastomas

These lesions are extremely rare epithelial tumors affecting the major salivary glands, usually the parotid and less often the submandibular gland^[3,31]. They generally occur perinatally, sometimes detected on an antenatal scan, as local swelling and less often as nevus sebaceous^[3,31,32].

Histopathologically, sialoblastomas are reminiscent of the embryonal epithelial anlage of the major salivary glands at various stages of development and cytodifferentiation, showing necrosis or cytological atypia beyond that expected for an embryonal epithelium^[31].

Reports on the imaging characteristics of sialoblastoma are limited. It manifests as a soft-tissue mass usually invasive to the adjacent bone and muscles^[3,33]. On CT, it is hypodense to the brain and isodense to muscle^[33]. On MRI, it is isointense to muscle on T1W images and shows higher intermediate signal intensity on T2W images, which suggests a high nucleus/cytoplasmic ratio belonging to blastema and possibly predictive of blastomas (Fig. 8a,b)^[33,34]. Intra-tumoral areas of necrosis and hemorrhage may be seen, probably due to minor trauma of the fragile tumor tissue during vaginal delivery. Post injection of contrast medium, enhancement is heterogeneous and weak (Fig. 8c)^[33,34].

In this age group, however, it should be remembered that the commonest lesion in the salivary glands, with predilection of the parotids, is the hemangioma. However, hemangiomas typically show hypervascularity on color Doppler ultrasound, uniform and intense enhancement post contrast injection on CT and MRI, and presence of flow voids on spin-echo MRI.

Sialoblastomas may become more anaplastic over time and are treated with surgery. Their clinical course is unpredictable and several recurrences post-operatively have been reported^[3,33].

Pleuropulmonary blastomas (PPBs)

PPBs are rare intra-thoracic pediatric malignant tumors that consist of primitive or immature-appearing mesenchyme, often rhabdomyosarcomatous, with non-neoplastic, presumably entrapped, epithelium. Because of their rare occurrence in childhood, primary pulmonary neoplasms are usually diagnosed with a significant delay, being confused with other neoplasms or pleural empyema^[35,36].

PPB usually occurs in children less than 5 years of age^[37], which present with non-specific respiratory distress, or signs of respiratory tract infection and spontaneous pneumothorax^[36,38]. A few cases of critical life-threatening presentation have been reported^[36].

PPB is classified into three subtypes: type 1 (in 14%), which is predominately macrocystic, type 3 (in 38%), which is predominately solid and type 2 (in 48%), which is mixed^[37,38]. The cystic type may be misdiagnosed and managed as a benign cyst or type IV congenital pulmonary airway malformation (CPAM). PPB has recently been recognized as distinct from pulmonary blastoma, which is a focal lung tumor seen predominantly in adults^[39].

The etiology of PPB remains unknown, but pathogenetic molecular abnormalities have been reported^[37]. PPB has not been included in any well-characterized syndromic disorder but approximately 25% of cases occur in a familial setting with high prevalence of other tumors, such as multilocular cystic nephromas, thyroid adenomas and carcinomas, sarcomas, medulloblastomas, germ cell tumors, and hematological diseases^[36,38,40].

Specific imaging findings to favor PPB are right-sided, pleural-based, peripherally located mass without chest wall invasion, that causes almost complete opacification of the hemithorax and mass effect, shows

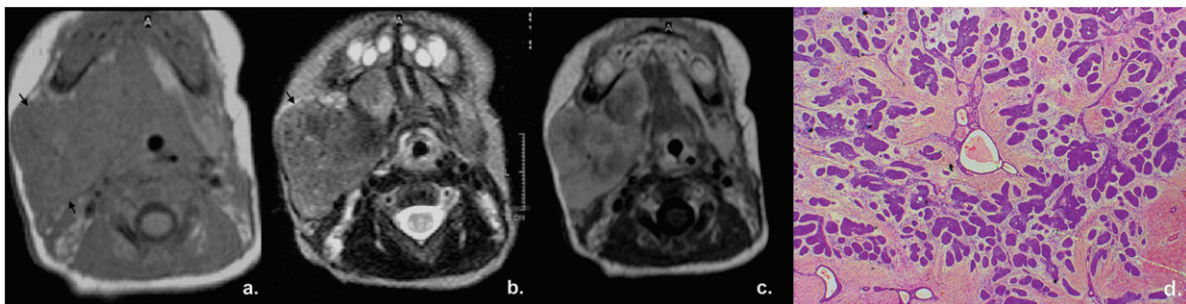


Figure 8 A 5-day-old female infant presented with swelling of the right cheek due to sialoblastoma. Axial MRI scans revealed a solid lesion in the right parotid region (arrows) which showed low signal on T1W (a), intermediate signal on T2W (b), heterogeneous and rather weak enhancement on T1W images post gadolinium (c), findings which make the diagnosis of hemangioma unlikely. (d) Photomicrograph demonstrating numerous islands of cellular blastematous tissue within a spindle cell stroma, with poorly formed ductular-type structures (H&E, original magnification $\times 100$).

heterogeneously low attenuation with no calcification, and may be associated with pleural effusion and pneumothorax (Fig. 9)^[36,38,39]. PPB, especially in children with type II or III, gives metastases mainly to the CNS and the skeletal system^[36].

Treatment is surgical excision followed by chemotherapy. Complete excision may be difficult in the presence of invasion in the adjacent vital mediastinal structures (Fig. 10)^[38]. PPBs along with rhabdomyosarcomas and rhabdoid tumors are considered the most aggressive

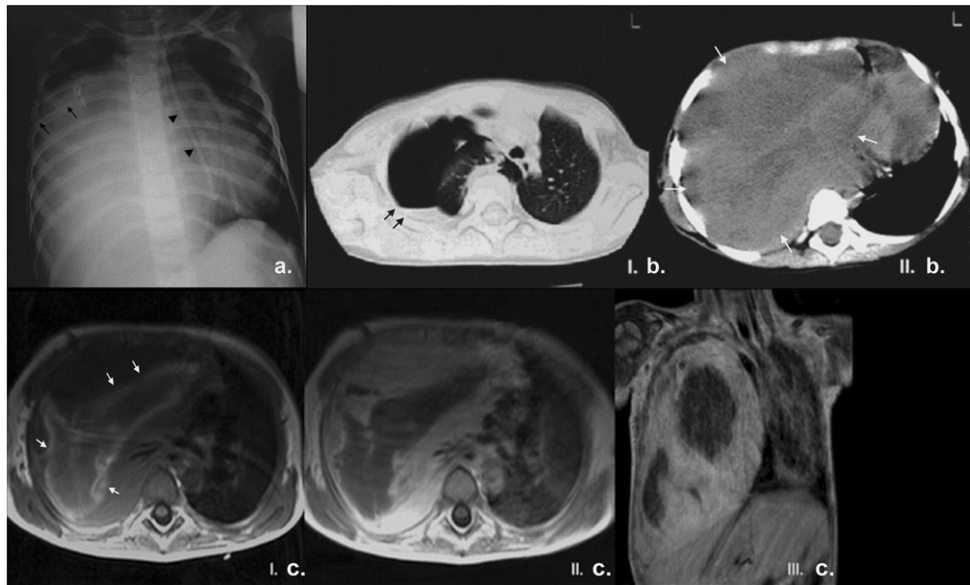


Figure 9 A 4-year-old boy with PPB presented to the local hospital with signs of lower tract infection. Ultrasound of the chest revealed hypoechoic material occupying the right pleural space, thought at the time to represent pleural empyema. (a) Plain film of the chest upon referral to our institution revealed opacification of almost the entire right hemithorax with loss of right hemidiaphragm, and mediastinal shift to the left (note the deviation of the nasogastric tube (arrowheads) placed high in position); there was no erosion or splaying of adjacent ribs. A right pleural drain had been inserted (arrows) but output was poor. (b) Unenhanced CT of the chest performed in the local hospital showed right hydropneumothorax (black arrows) – lung window settings (I) – and a large right-sided heterogeneous low attenuation mass which occupied the right hemithorax (white arrows), caused mediastinal shift to the left with absence of chest wall invasion – soft tissue settings (II). These findings are considered typical of PPB. (c) MRI of the chest confirmed the presence of a heterogeneous mass in the right hemithorax with low signal intensity on T1W images, linear, possibly hemorrhagic, areas of increased signal intensity (white arrows) (I), and peripheral regions of contrast enhancement on axial and coronal T1W images post gadolinium (II and III respectively).

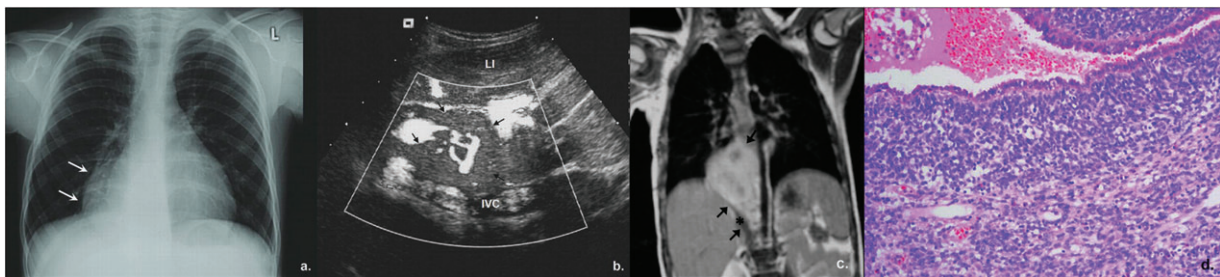


Figure 10 A 3.5-year-old girl with history of previously resected right-sided PPB. (a) On follow-up chest X-ray, right paracardial opacity was noted (arrows). A solid, pleural-based, peripheral vascular mass (arrows) was confirmed on US. (b) A right parasagittal image of the upper abdomen (LI, liver; IVC, inferior vena cava) and (c) MRI (coronal T1W image post gadolinium, * indicates diaphragm displaced inferiorly). Close proximity of the mass to the IVC was noted. (d) Pathology showed relapse of the previously resected PPB. Photomicrograph demonstrating surface epithelium overlying stroma which is extensively infiltrated by a 'small ovoid cell' tumor, characteristic of PPB (H&E, original magnification $\times 100$).

pulmonary neoplasms and radiologists should raise the possibility of PPB in the differential diagnosis of a chest mass in the appropriate-age child^[35].

Pancreatoblastomas

These are rare primary neoplasms of the pancreas, but together with solid and papillary epithelial neoplasms they represent the commonest pancreatic tumors in the pediatric population^[41,42]. Histologically, pancreatoblastoma resembles the incompletely differentiated acini of the fetal pancreatic tissue at 7 weeks gestational age^[42,43].

Two categories have been reported on the basis of the anatomic origin of pancreatoblastomas: those arising from the ventral anlage of the pancreas, which are the right-sided, well-encapsulated tumors with no calcifications and good prognosis, and those arising from the dorsal anlage, the left-sided tumors^[42,44]. Dorsal anlage tumors contain islet cells, are infiltrative, show calcification and have a poor prognosis.

The age group affected is usually between 1 and 8 years, with a mean age of about 5 years^[42,43]. There is male and East Asian predominance^[45]. The association of the congenital form of cystic pancreatoblastoma with Beckwith–Wiedmann syndrome, with alterations in the APC/ β -catenin signaling pathway, has been described^[46].

Pancreatoblastomas grow slowly, acquire large size at presentation which makes it difficult to identify the organ of origin and differentiate from other abdominal pediatric malignancies. They cause symptoms from mass effect, or endocrine syndromes due to tumor adrenocorticotrophic secretion and anemia due to duodenal and vascular invasion^[43,45]. Peritoneal and omental dissemination with ascites and distal metastases more commonly to the liver, and less often to the lung, bones, posterior mediastinum and the neck lymph nodes may be seen (Fig. 11)^[44,45].

Imaging can be suggestive of pancreatoblastomas. They present as well-defined, lobulated, heterogeneous masses, with necrosis and/or calcification, usually arising from the body and/or tail of the pancreas or involving the entire organ, rather than being universally located in the pancreatic head^[45]. Since pancreatoblastomas are of soft and gelatinous consistency, they rarely cause biliary or duodenal obstruction, but they may encase adjacent vessels, which makes their distinction from neuroblastoma difficult^[44,45,47].

On US, pancreatoblastomas show mixed or low echogenicity, sometimes containing small fluid areas (Fig. 11a,b). On CT (Fig. 11c,d), they are usually well-defined, hypodense lesions which show mild enhancement and internal enhancing septations. Calcifications within the lesion are either rim-like or clustered. On MRI, pancreatoblastomas usually have non-specifically

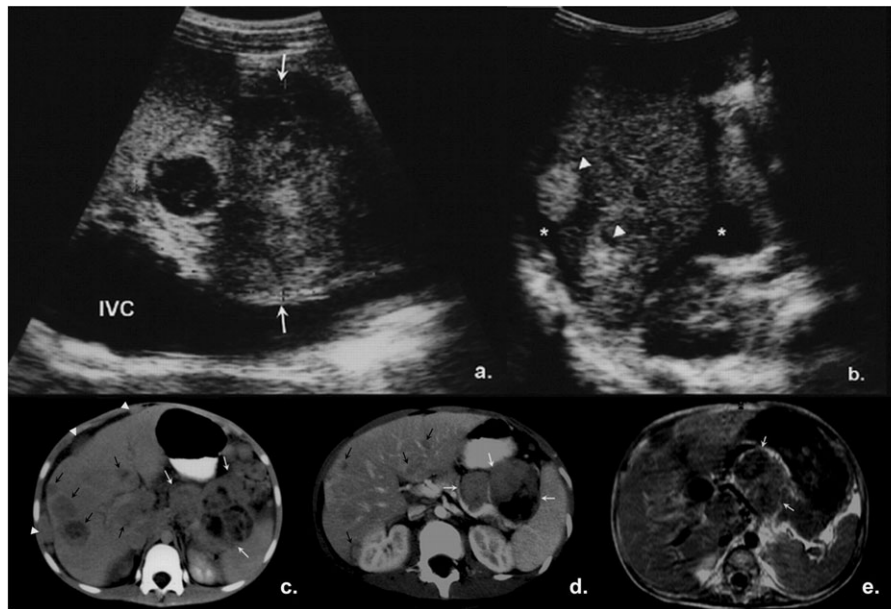


Figure 11 Appearances of pancreatoblastoma on US (a,b), CT (c,d) and MRI (e). Large heterogeneous mass with cystic areas at the pancreatic head (white arrows) (parasagittal section (a), IVC, inferior vena cava). Subcapsular liver metastases (arrowheads) and ascites (*), indicative of peritoneal seeding (axial section (b)). Large lobulated masses within the pancreatic body and tail (white arrows (c)–(e)). They are heterogeneous with hypodense areas on enhanced CT image (d) and of low signal intensity on T1W axial MRI images (c). Liver metastases of different sizes are recognized as multiple hypodense lesions on CT (black arrows, (c,d) while the presence of subcapsular liver nodules indicates peritoneal seeding (arrowheads (b,c)).

low to intermediate signal on T1W images (Fig. 11e) and high signal on T2W images, and may show enhancement^[42,45,47].

Overall pancreatoblastomas are considered malignant due to their capacity to metastasize; however, 75% are resectable and only 14% progress after resection^[46].

Pineoblastomas or pinealoblastomas

These lesions arise from the pineal parenchymal cell, the pineocyte, account for only 15% of masses of the pineal region and represent extremely malignant embryonal neoplasms composed of primitive pineal cells that present most commonly in children. They bear appropriately the suffix 'blastoma', being part of the larger group of PNETs, which histologically show a relationship to primitive, 'blastic' CNS elements^[2]. They cause obstruction of the aqueduct of Sylvius and hydrocephalus, with compression of the midbrain tegmentum. Abnormal neuro-ophthalmologic findings and neuroendocrine dysfunction is a known association. Pineoblastoma may occur in a background of genetic predisposition with familial bilateral retinoblastomas, an association known as 'trilateral retinoblastoma'^[48].

On unenhanced CT, pineoblastoma shows areas of increased cellularity which are demonstrated as hyperdense regions, and features of aggressive infiltration (Fig. 12a). MRI depicts a lobulated, invasive, solid

lesion which enhances avidly with contrast. Signal intensity varies but pineoblastomas are essentially isointense to grey matter on T2W images, possibly related to the known paucity of cytoplasm and their dense cellularity (Fig. 12)^[49]. Reports in adults with pineoblastoma outline the restricted water diffusion the lesions show due to their high cellularity in diffusion-weighted MRI images^[50]. Pineoblastomas are given grade IV WHO classification, implying the highest degree of malignancy, usually show rapid recurrence and cerebrospinal dissemination, and are associated with a poor prognosis^[2,51].

Medullomyoblastomas

They are rare embryonal tumors of the CNS, variants of medulloblastomas that show a degree of rhabdomyoblastic differentiation^[52]. They arise exclusively in the infratentorial compartment and occur in children less than 10 years of age with male predominance.

Tumors exhibit hypercellularity on imaging studies, show variable enhancement and may contain necrotic areas. On CT, they present as hyperdense cerebellar masses frequently associated with hydrocephalus (Fig. 13). Biphasic nodularity, expressed as discrete T2W hypointense, CT hyperdense enhancing or T2W hyperintense, CT hypodense non-enhancing nodular foci, has been reported as a possible diagnostic feature of medullomyeloblastomas^[52].

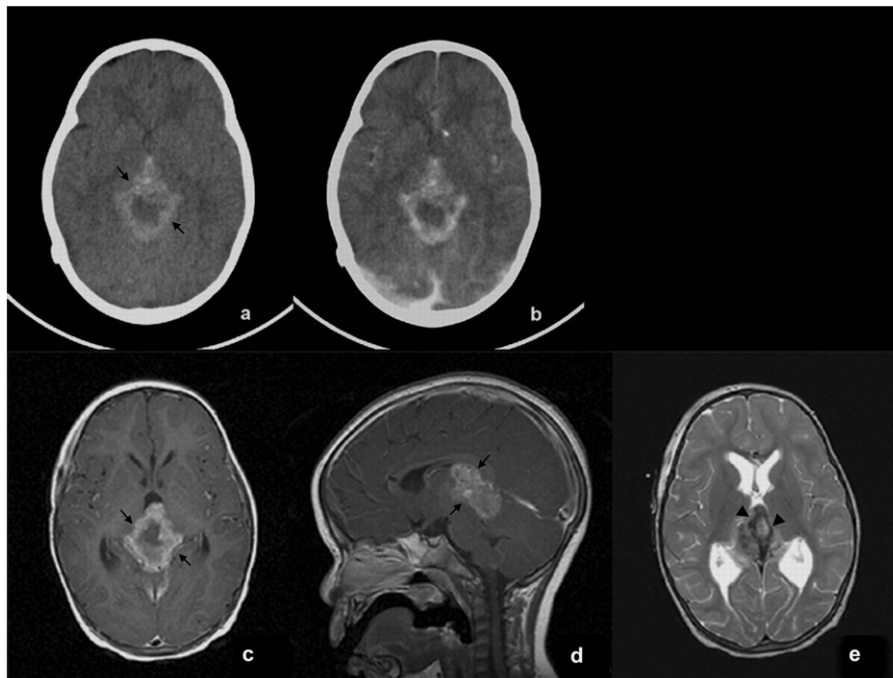


Figure 12 CT (a,b) and MRI (c–e) images through the brain in a 2.5-year-old girl with pineoblastoma. An infiltrative mass in the pineal region is demonstrated (black arrows), with hyperdense indistinct borders on unenhanced CT (a), suggestive of increased cellularity. Post injection of contrast (b), there is peripheral enhancement of the mass evident on CT (b) and MRI (T1W axial (c) and sagittal (d) post gadolinium images). On T2W images, there are areas of low signal intensity suggestive of hypercellularity (arrowheads) (e).

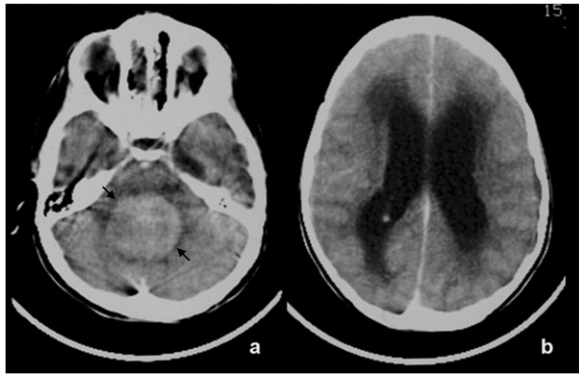


Figure 13 Axial enhanced CT scans through the brain in a 3.5-year-old girl with medulloblastoma who presented signs of hydrocephalus. A hyperdense midline cerebellar mass is seen (arrows, a), compressing the brain stem anteriorly and causing obstructive hydrocephalus with subependymal edema (b).

Treatment strategy is similar to that of medulloblastoma and includes surgery with chemotherapy and radiotherapy. Overall prognosis is poor.

Summary

We have presented the radiological features of several entities within this group of tumors that individually represent less than 1% of all pediatric neoplasms. Since these neoplasms are extremely rare, most centers will only encounter isolated cases and the suggestive imaging features described may help the radiologist to consider them in the differential diagnosis.

Acknowledgements

We would like to express our sincere thanks to Dr D. Roebuck for Fig. 11.

References

- [1] Maris JM, Denny CT. Focus on embryonal malignancies. *Cancer Cell* 2002; 2: 447–50. doi:10.1016/S1535-6108(02)00206-4. PMID:12498713.
- [2] Vogel H, Fuller GN. Primitive neuroectodermal tumors, embryonal tumors, and other small cell and poorly differentiated malignant neoplasms of the central and peripheral nervous systems. *Ann Diagn Pathol* 2003; 7: 387–98. doi:10.1016/j.anndiagnpath.2003.09.007. PMID:15018124.
- [3] Brandwein M, Al Naeif NS, Manwani D, et al. Sialoblastoma: clinicopathological/immunohistochemical study. *Am J Surg Pathol* 1999; 23: 342–8. doi:10.1097/0000478-199903000-00015. PMID:10078927.
- [4] Ellison D. Classifying the medulloblastoma: insights from morphology and molecular genetics. *Neuropathol Appl Neurobiol* 2002; 28: 257–82. doi:10.1046/j.1365-2990.2002.00419.x. PMID:12175339.
- [5] Harrer J, Hammon G, Wagner T, Bolkenius M. Lipoblastoma and lipoblastomatosis: a report of two cases and review of the literature. *Eur J Pediatr Surg* 2001; 11: 342–9. doi:10.1055/s-2001-18544. PMID:11719876.

- [6] Moholkar S, Sebire NJ, Roebuck DJ. Radiological-pathological correlation in lipoblastoma and lipoblastomatosis. *Pediatr Radiol* 2006; 36: 851–6. doi:10.1007/s00247-006-0175-5. PMID:16775739.
- [7] O'Donnell KA, Caty MG, Allen JE, Fisher JE. Lipoblastoma: better termed infantile lipoma? *Pediatr Surg Int* 2000; 16: 458–61. doi:10.1007/s003839900252. PMID:10955594.
- [8] Chung EB, Enzinger FM. Benign lipoblastomatosis. An analysis of 35 cases. *Cancer* 1973; 32: 482–492. doi:10.1002/1097-0142(197308)32:2<482::AID-CNCR2820320229>3.0.CO;2-E. PMID:4353020.
- [9] Dy JS, Fuchs A, Palmer LS. Benign intracrotal lipoblastoma in a child. *Urology* 2007; 70: 372. doi:10.1016/j.urology.2007.04.001.
- [10] Ozkal E, Erongun U, Cakir B, Acar O, Uygun A, Bitik M. CT and MR imaging of vertebral osteoblastoma. A report of two cases. *Clin Imaging* 1996; 20: 37–41. doi:10.1016/0899-7071(94)00074-3. PMID:8846307.
- [11] LaBan MM, Riutta JC. 'Occult' roentgenographic osteoblastoma of the cervical spine. *Am J Phys Med Rehabil* 2003; 82: 820–3. doi:10.1097/01.PHM.0000087457.02231.FE.
- [12] Arkader A, Dormans JP. Osteoblastoma in the skeletally immature. *J Pediatr Orthop* 2008; 28: 555–60. PMID:18580372.
- [13] Azouz EM. Magnetic resonance imaging of benign bone lesions: cysts and tumors. *Top Magn Reson Imaging* 2002; 13: 219–29. doi:10.1097/00002142-200208000-00003. PMID:12409690.
- [14] Shaikh MI, Saifuddin A, Pringle J, Natali C, Sherazi Z. Spinal osteoblastoma: CT and MR imaging with pathological correlation. *Skeletal Radiol* 1999; 28: 33–40. doi:10.1007/s002560050469. PMID:10068073.
- [15] Cervoni L, Innocenzi G, Raguso M, Salvati M, Caruso R. Osteoblastoma of the calvaria: report of two cases diagnosed with MRI and clinical review. *Neurosurg Rev* 1997; 20: 51–4. doi:10.1007/BF01390526. PMID:9085288.
- [16] Erler K, Yildiz C, Demiralp B, Ozdemir MT, Basbozkurt M. Chondroblastoma of the distal femur. A case report. *Acta Orthop Belg* 2003; 69: 467–72. PMID:14648960.
- [17] Ilaşlan H, Sundaram M, Unni KK. Vertebral chondroblastoma. *Skeletal Radiol* 2003; 32: 66–71. doi:10.1007/s00256-003-0687-0. PMID:14586575.
- [18] Jain M, Kaur M, Kapoor S, Arora DS. Cytological features of chondroblastoma: a case report with review of the literature. *Diagn Cytopathol* 2000; 23: 348–50. doi:10.1002/1097-0339(200011)23:5<348::AID-DC13>3.0.CO;2-2. PMID:11074632.
- [19] Masui F, Ushigome S, Kamitani K, Asanuma K, Fujii K. Chondroblastoma: a study of 11 cases. *Eur J Surg Oncol* 2002; 28: 869–74. doi:10.1053/ejso.2002.1276. PMID:12477480.
- [20] Garin IE, Wang EH. Chondroblastoma. *J Orthop Surg (Hong Kong)* 2008; 16: 84–7. PMID:18453666.
- [21] Ramappa AJ, Lee FY, Tang P, Carlson JR, Gebhardt MC, Mankin HJ. Chondroblastoma of bone. *J Bone Joint Surg Am* 2000; 82-A: 1140–5. PMID:10954104.
- [22] Chung OM, Yip SF, Ngan KC, Ng WF. Chondroblastoma of the lumbar spine with cauda equina syndrome. *Spinal Cord* 2003; 41: 359–64. doi:10.1038/sj.sc.3101458. PMID:12746743.
- [23] Maezawa K, Nozawa M, Takagi T, Imai D, Shitoto K, Kurosawa H. Rotational acetabular osteotomy for benign chondroblastoma of the femoral head. A case report. *J Bone Joint Surg Am* 2005; 87: 1358–62. doi:10.2106/JBJS.D.02457. PMID:15930549.
- [24] Hande AM, Nagpal RD. Cerebellar haemangioblastoma with extensive dissemination. *Br J Neurosurg* 1996; 10: 507–11. doi:10.1080/02688699647186. PMID:8922714.
- [25] Quadery FA, Okamoto K. Diffusion-weighted MRI of haemangioblastomas and other cerebellar tumours. *Neuroradiology* 2003; 45: 212–19. PMID:12687303.
- [26] Isaacs H, Jr. Perinatal (fetal and neonatal) germ cell tumors. *J Pediatr Surg* 2004; 39: 1003–13. doi:10.1016/j.jpedsurg.2004.03.045. PMID:15213888.

- [27] Livadas S, Mavrou A, Sofocleous C, Vliet-Constantinidou C, Dracopoulou M, Dacou-Voutetakis C. Gonadoblastoma in a patient with del(9)(p22) and sex reversal: report of a case and review of the literature. *Cancer Genet Cytogenet* 2003; 143: 174–7. doi:10.1016/S0165-4608(02)00849-X. PMID:12781454.
- [28] Lau YF. Gonadoblastoma, testicular and prostate cancers, and the TSPY gene. *Am J Hum Genet* 1999; 64: 921–7. doi:10.1086/302353. PMID: 10090875.
- [29] Obata NH, Nakashima N, Kawai M, Kikkawa F, Mamba S, Tomoda Y. Gonadoblastoma with dysgerminoma in one ovary and gonadoblastoma with dysgerminoma and yolk sac tumor in the contralateral ovary in a girl with 46XX karyotype. *Gynecol Oncol* 1995; 58: 124–128. doi:10.1006/gyno.1995.1195. PMID:7789879.
- [30] Hatano T, Yoshino Y, Kawashima Y, *et al.* Case of gonadoblastoma in a 9-year-old boy without physical abnormalities. *Int J Urol* 1999; 6: 164–6. doi:10.1046/j.1442-2042.1999.06331.x. PMID:10226831.
- [31] Mostafapour SP, Folz B, Barlow D, Manning S. Sialoblastoma of the submandibular gland: report of a case and review of the literature. *Int J Pediatr Otorhinolaryngol* 2000; 53: 157–61. doi:10.1016/S0165-5876(00)00311-6. PMID:10906522.
- [32] Garrido A, Humphrey G, Squire RS, Nishikawa H. Sialoblastoma. *Br J Plast Surg* 2000; 53: 697–9. doi:10.1054/bjps.2000.3452. PMID:11090328.
- [33] Yekeler E, Dursun M, Gun F, *et al.* Sialoblastoma: MRI findings. *Pediatr Radiol* 2004; 34: 1005–7. doi:10.1007/s00247-004-1286-5. PMID:15278323.
- [34] Som PM, Brandwein M, Silvers AR, Rothschild MA. Sialoblastoma (embryoma): MR findings of a rare pediatric salivary gland tumor. *AJNR Am J Neuroradiol* 1997; 18: 847–50. PMID: 9159361.
- [35] Cohen MC, Kaschula RO. Primary pulmonary tumors in childhood: a review of 31 years' experience and the literature. *Pediatr Pulmonol* 1992; 14: 222–232. doi:10.1002/ppul.1950140405. PMID:1336597.
- [36] Piastra M, Ruggiero A, Caresta E, *et al.* Critical presentation of pleuropulmonary blastoma. *Pediatr Surg Int* 2005; 21: 223–6. doi:10.1007/s00383-004-1325-1. PMID:15756566.
- [37] Bini A, Ansaloni L, Grani G, *et al.* Pulmonary blastoma: report of two cases. *Surg Today* 2001; 31: 438–42. doi:10.1007/s005950170136. PMID:11381509.
- [38] Kukkady A, Upadhyay V, Pease PW, Chan YF. Pleuropulmonary blastoma: four cases. *Pediatr Surg Int* 2000; 16: 595–8. doi:10.1007/s003830000359. PMID:11149404.
- [39] Naffaa LN, Donnelly LF. Imaging findings in pleuropulmonary blastoma. *Pediatr Radiol* 2005; 35: 387–91. doi:10.1007/s00247-004-1367-5. PMID:15657793.
- [40] Roque L, Rodrigues R, Martins C, *et al.* Comparative genomic hybridization analysis of a pleuropulmonary blastoma. *Cancer Genet Cytogenet* 2004; 149: 58–62. doi:10.1016/S0165-4608(03)00284-X. PMID:15104284.
- [41] Nijs E, Callahan MJ, Taylor GA. Disorders of the pediatric pancreas: imaging features. *Pediatr Radiol* 2005; 35: 358–73. doi:10.1007/s00247-004-1326-1. PMID:15536562.
- [42] Chung EM, Travis MD, Conran RM. Pancreatic tumors in children: radiologic-pathologic correlation. *Radiographics* 2006; 26: 1211–38. doi:10.1148/rg.264065012. PMID:16844942.
- [43] Sheng L, Weixia Z, Longhai Y, Jinming Y. Clinical and biologic analysis of pancreatoblastoma. *Pancreas* 2005; 30: 87–90. PMID:15632705.
- [44] Gupta AK, Mitra DK, Berry M, Dinda AK, Bhatnagar V. Sonography and CT of pancreatoblastoma in children. *AJR Am J Roentgenol* 2000; 174: 1639–41. PMID: 10845499.
- [45] Roebuck DJ, Yuen MK, Wong YC, Shing MK, Lee CW, Li CK. Imaging features of pancreatoblastoma. *Pediatr Radiol* 2001; 31: 501–6. doi:10.1007/s002470100448. PMID:11486805.
- [46] Barenboim-Stapleton L, Yang X, Tsokos M, *et al.* Pediatric pancreatoblastoma: histopathologic and cytogenetic characterization of tumor and derived cell line. *Cancer Genet Cytogenet* 2005; 157: 109–117. doi:10.1016/j.cancergencyto.2004.05.017. PMID:15721631.
- [47] Montemarano H, Lonergan GJ, Bulas DI, Selby DM. Pancreatoblastoma: imaging findings in 10 patients and review of the literature. *Radiology* 2000; 214: 476–82. PMID: 10671596.
- [48] Plowman PN, Pizer B, Kingston JE. Pineal parenchymal tumours: II. On the aggressive behaviour of pineoblastoma in patients with an inherited mutation of the RB1 gene. *Clin Oncol (R Coll Radiol)* 2004; 16: 244–7. doi:10.1016/j.clon.2003.12.005. PMID:15214647.
- [49] Korogi Y, Takahashi M, Ushio Y. MRI of pineal region tumors. *J Neurooncol* 2001; 54: 251–61. doi:10.1023/A:1012773727022. PMID:11767291.
- [50] Gasparetto EL, Cruz Jr LC, Doring TM, *et al.* Diffusion-weighted MR images and pineoblastoma: diagnosis and follow-up. *Arq Neuropsiquiatr* 2008; 66: 64–8. doi:10.1590/S0004-282X2008000100015. PMID:18392417.
- [51] Hirato J, Nakazato Y. Pathology of pineal region tumors. *J Neurooncol* 2001; 54: 239–49. doi:10.1023/A:1012721723387. PMID:11767290.
- [52] Helton KJ, Fouladi M, Boop FA, *et al.* Medulloblastoma: a radiographic and clinicopathologic analysis of six cases and review of the literature. *Cancer* 2004; 101: 1445–54. doi:10.1002/cncr.20450. PMID:15368333.